

**METHOD OF DETUNING FROM RESONANCE MODES FOR ROTORS IN ACTIVE  
 MAGNETIC BEARINGS WITH NONLINEAR FORCE CHARACTERISTICS**

**G. Martynenko**<sup>1</sup>  
 National Technical  
 University "Kharkiv  
 Polytechnic Institute",  
 Kharkiv, Ukraine

ABSTRACT

In the report, the investigator offers a method of reducing the amplitude of vibrations of turbo machinery rotors with passive and active magnetic bearings (AMB) in resonances and resonance zones corresponding to one of the critical speeds from zero to working rotational speeds. The method is based on the ability to vary the nonlinear force characteristic and the damping properties of AMB by changing the electric parameters of the electromagnet circuits.

**INTRODUCTION**

One of the methods of reducing vibrations in rotor machines in different applications is to use the self-centering rotor effect, which is manifested during supercritical operation [1]. The model in Fig. 1 illustrates the physical essence of this phenomenon. It implies that, when a unbalanced rotor reaches the critical rotational speed  $\omega$ , the direction of deflection  $y$  and eccentricity  $e$  become opposite, the centre of mass  $C$  is displaced and occupies a position between the geometric centre  $O$  and axis of rotation  $O^*z$  (Fig. 1a). Further rotational speed increasing makes the absolute value of shaft deflection approach eccentricity  $e$  (Fig. 1b), i.e. the centre of mass approaches the axis of rotation. For rotors in rigid supports, the value of the first critical velocity is comparatively big. In this case, the zone of working rotational speeds can be located at an insufficient distance from the critical speed one to reduce rotor vibration amplitudes (Fig. 1b).

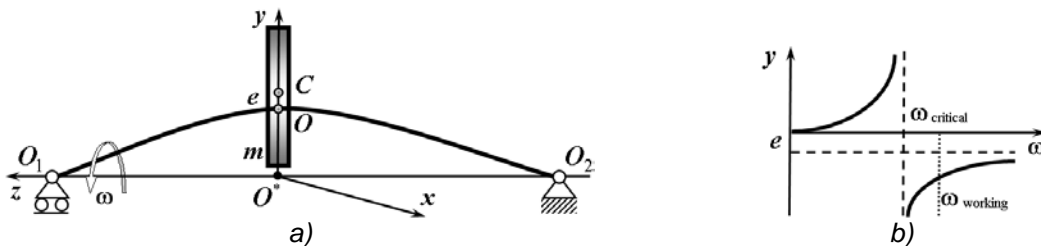


Fig. 1 Rotor model (a) and shaft deflection vs. rotational frequency (b)

In practice, one of two methods is used to offset the rotor machine from resonance modes. The first method implies displacement of increased vibration zones in the increasing direction so that the entire range of working rotational speeds is located before the first critical speed (rigid rotor). The second method implies machine operation in supercritical areas (a flexible rotor). In this case, it is necessary to reduce the values of the first critical rotational speed, i.e. the increased vibration zone threshold, and at the same time ensure safe transition through critical speeds in the range up to maximal working rotational speeds [1]. This is achieved by reducing the stiffness of the "rotor-support" dynamical system. To do this, the rotors are mounted in flexible supports (FS) with specified stiffness [1]. The vibration amplitudes can be reduced with the help of elastic-dampening supports (EDS) by introducing artificial dampeners into their design. This will decrease the amplitudes of resonance vibrations; however, machine efficiency will drop.

Fig. 2 shows rotor vibration modes in different supports corresponding to the first three critical

<sup>1</sup> Corresponding author. Email [gmartynenko@kpi.kharkov.ua](mailto:gmartynenko@kpi.kharkov.ua)

rotational speeds. For extremely yielding supports, the rotor passes the first two critical speeds with formation of cylindrical and conical precession (Fig. 2a). A curved vibration mode corresponds to the third critical speed.

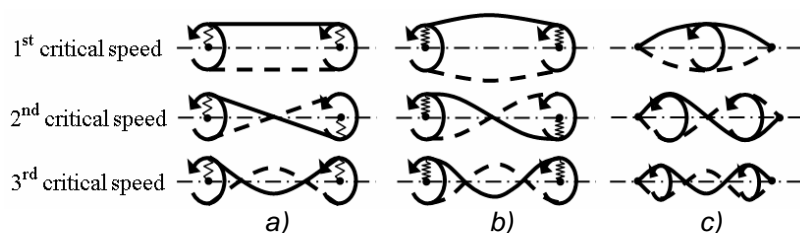


Fig. 2 Lateral vibration modes of rotors in different supports:  
a) extremely yielding, b) yielding, c) rigid

The most common vibrations of rotors are those caused by static and moment imbalance. The amplitudes of such vibrations can be reduced dramatically by utilising the properties of a stiff rotor in an ES [1]. However, there are also other kinds of hazardous vibrations directly related to using mechanical ES. They are autovibrations caused by the properties of the oil film in sleeve bearings; different kinds of nonlinear vibrations related to nonlinearity of the force characteristics of roller bearings as preloaded systems, and others.

When a rotor is mounted in an ES, troubles can occur during rotor acceleration and its passing through critical speeds when the rotor vibrates as a rigid body [1]. The paper offers a method of passing such increased vibration zones by a short-time change of ES stiffness during rotor acceleration or its rundown, i.e. stiffness control as a function of rotational speed. Then the ES force characteristics will be adaptive, allowing for offsetting the “rotor in ES” system from critical speeds over the entire range from zero to working rotational speeds of the rotor machine. Active magnetic bearings (AMB) are suggested to be used as an ES with variable stiffness. In these bearings, rotor position stability is ensured by a control system (CS) with negative feedback [2]. The force characteristics of these bearings, in contrast to those of mechanical ES, can change by varying the electric parameters (voltages or control currents) [3]. By changing the values of active resistances in AMB circuits, one can control damping by increasing it only in the resonance zones. In this case, AMB will be an EDS with variable parameters.

Yet another feature of AMBs to be mentioned is the nonlinear dependence of their force characteristics on displacement of rotor support sections (i.e. on the gap between the journal and stator poles) as well as on the currents in the pole coil windings. They change as a function of rotor position defined by the control system according to a preset law.

## 1. DESCRIPTION OF THE METHOD OF OFFSETTING A ROTOR IN AN AMB FROM CRITICAL ROTATIONAL SPEEDS DURING ACCELERATION AND RUNDOWN

The suggested method of offsetting the rotor from critical speeds (passing the resonances) during acceleration or rundown implies that the control system (CS) changes rapidly the stiffness and/or damping parameters of magnetic bearings. Besides having position sensors, the CS also has an angular speed sensor [3]. Fig. 3 is the structural diagram of a system version for a radial AMB. The stiffness properties of the AMB can be varied within a certain range of angular speeds by changing the values of control voltages  $u_{c1}, \dots, u_{c4}$ . This results in a change of average currents  $i_{c1}, \dots, i_{c4}$  (bias currents) in the windings of electromagnets and allows changing the force characteristics of the support [4]. The AMB damping properties can be increased for a short time by increasing the active resistances  $r_{c1}, \dots, r_{c4}$  in the circuits of the electromagnets in the zone of rotor critical rotational speeds. This will reduce the amplitudes of resonance vibrations [4].

The algorithm of operation of the control system suggested assumes prior selection of two (or more) operating conditions. In the first condition (the design one), the AMB force characteristics should ensure required motion stability of the supercritical rotor in a certain range of angular velocities spanning the working rotational speeds. The second operating condition assumes operation with greater (lesser) support stiffness as compared to the first case. The stiffness should be such that the first critical speeds of the rotor be higher (lower) as compared to the system operating in the first (design) condition. Rotor acceleration is initiated in the first operating condition. Then, as the rotor approaches the critical zones, the operating condition is switched to the second one, and when the resonance areas of the first operating condition have been passed, the operating condition is switched back to the first (design) one. If there are several resonances prior to onset of working rotational speeds, successive switching from the first operating condition to the second one and vice versa will

exclude completely vibrations with increased amplitudes. During rotor rundown, the process of resonance passing is similar. In general, there can be several such operating conditions. In this case, switching between them should take place according to a predefined program.

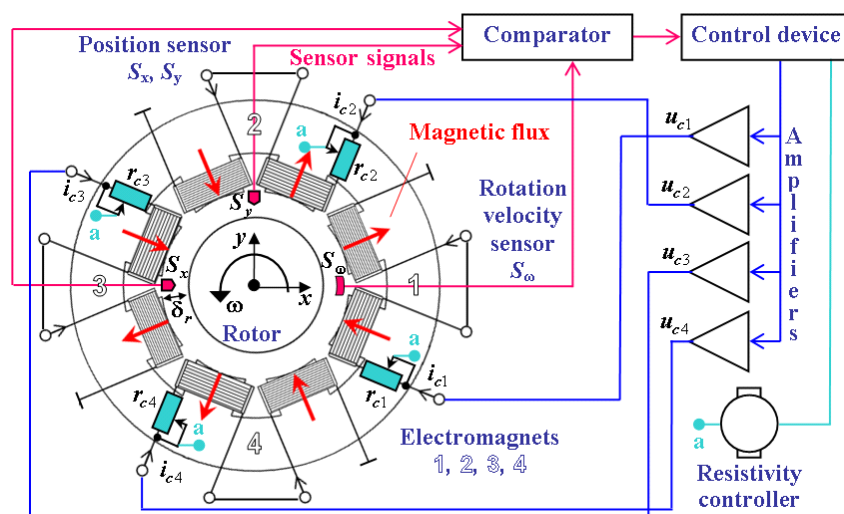


Fig. 3 Structural diagram of a CS for controlling rotor motion in a radial AMB with controlled stiffness and damping parameters

Fig. 4 is a schematic presentation of how the supercritical rotor reaches working rotational speeds and passes through the first resonance (critical speed). The diagram shows the dependence of the amplitude of the first forced vibrations harmonic ( $A_1$ ) on the frequency ( $\omega$ ) of the harmonic driving force for a stiff AMB force characteristic.  $A_1'$  and  $A_1''$  designate the resonance curves for different stiffness values, which are ensured by different values of average currents or bias currents. The resonance curve  $A_1''$  corresponds to bigger stiffness values, and curve  $A_1'$  is the amplitude-frequency response (AFR) of the design operating condition. The dashed lines in Fig. 4 are skeleton curves  $\omega_0'$  and  $\omega_0''$  corresponding to different stiffness values. Solid lines designate the resulting system AFR obtained when using the method proposed. It is implemented by passing from one resonance curve  $A_1'$  to another one  $A_1''$  by changing the stiffness of magnetic bearings in a preset range  $[\omega_{1min}, \omega_{1max}]$ . In this case, the maximum values of vibration amplitudes  $A_{1max}$  are significantly smaller than the maximums  $A_{1max}'$  and  $A_{1max}''$  of both resonance curves  $A_1'$  and  $A_1''$ .

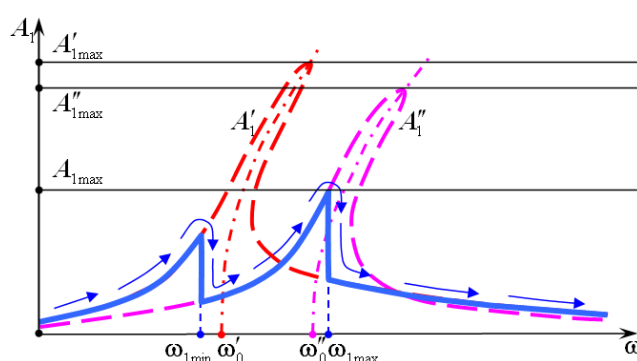


Fig. 4 Schematic presentation of the AFR of a rotor in an AMB with controlled stiffness

The vibration amplitude near the resonance can also be reduced by increasing the damping in the system. This is achieved by increasing the active resistances in the circuits of the coils of the AMB electromagnets (Fig. 4, curve  $A_1''$ ) [4]; however, this extends the resonance zone and results in additional energy consumption.

## 2. METHOD VALIDATION WITH NUMERICAL SIMULATION

To validate the functionality of the method suggested, a series of numerical experiments for a model of a magnetic suspension of a small-size high-speed rotor were conducted. Such a rotor suspension scheme can be suggested for application, for example, in rotors of expansion-compression units.

## 2.1 Mathematical model of the dynamics of a rigid rotor in magnetic bearings

Fig. 5 visualises the design model of a combined magnetic suspension, where  $O^*xyz$  are fixed right-hand Cartesian coordinates;  $O_1(x_1, y_1, z_1), O_2(x_2, y_2, z_2)$  are centres of support sections of the rotor in radial magnetic bearings in permanent ring magnets (MBPRM) located at distances  $l_1, l_2$  from the centre of mass  $C$ ;  $O_3(x_3, y_2, z_3)$  is the centre of the rotor support section in the axial AMB (disk centre of mass);  $u_{c1}, u_{c2}$  are control voltages applied across the windings of the axial AMB;  $i_{c1}, i_{c2}$  are currents in the windings of the axial AMB;  $e, \gamma$  are linear and angular eccentricities; and  $\omega$  is rotor angular speed.

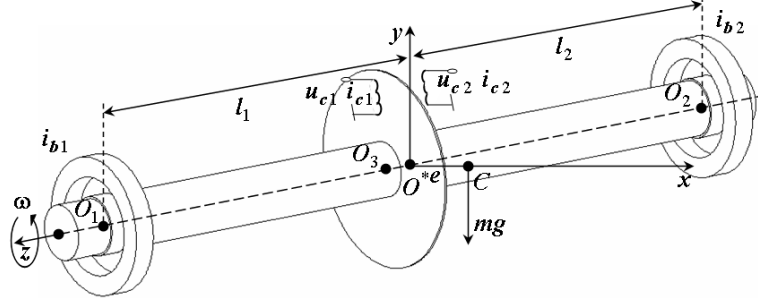


Fig. 5 Design model of a rotor in AMB with controlled stiffness

This combined magnetic suspension uses magnetic bearings shown in Fig. 6. The radial supports here are self-aligning MBPRM mounted in opposition to compensate for the axial force introduced by them. Their additional bias winding serves for implementing stiffness control. The axial support is a double-side action AMB. Fig. 6a shows the radial magnetic forces in MBPRM vs. rotor radial displacement at different values of parameters:  $F_{M0}$  at  $i_{b1,2}=0$ ,  $F_{M1}$  at  $i_{b1,2}=\pm 10$  A ( $w=150$ ),  $F_{M2}$  at  $i_{b1,2}=\pm 3.5$  A ( $w=500$ ) and  $F_{M3}$  at  $i_{b1,2}=\pm 1.3$  A ( $w=1,500$ ), where  $w$  is number of turns in windings [3]. Fig. 6b shows the axial magnetic forces vs. axial rotor displacement at different maximum voltage values  $U_0$  applied across AMB windings according to the preset control algorithm  $u_{c1}(z_3), u_{c2}(z_3)$  [3].

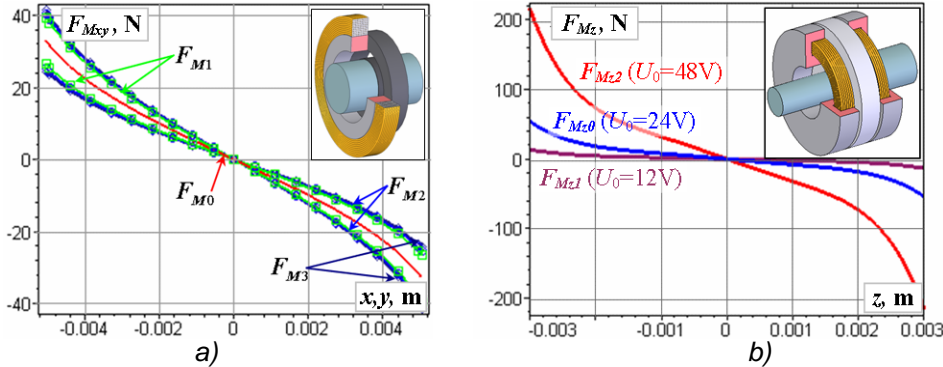


Fig. 6 Forces vs. displacements of rotor support sections in an experimental model: a) radial MBPRM with permanent magnets and an additional bias winding, b) double-sided action AMB

The dynamics of a rigid rotor in a combined magnetic suspension is described mathematically by a system of five differential equations, nonlinear with respect to generalised coordinates  $x_1, x_2, y_1, y_2, z_3$  and their time derivatives [5]:

$$\begin{cases} m_{11}\ddot{x}_1 + m_{12}\ddot{x}_2 + m_{13}\omega(\dot{y}_1 - \dot{y}_2) + b_{x1}\dot{x}_1 + f_{x1}(x_1, \dots, \ddot{z}_3) = F_{M_x}(x_1, y_1) + Q_{x1} + H_{x1}(t), \\ m_{22}\ddot{x}_2 + m_{12}\ddot{x}_1 - m_{13}\omega(\dot{y}_1 - \dot{y}_2) + b_{x2}\dot{x}_2 + f_{x2}(x_1, \dots, \ddot{z}_3) = F_{M_y}(x_1, y_1) + Q_{x2} + H_{x2}(t), \\ m_{11}\ddot{y}_1 + m_{12}\ddot{y}_2 - m_{13}\omega(\dot{x}_1 - \dot{x}_2) + b_{y1}\dot{y}_1 + f_{y1}(x_1, \dots, \ddot{z}_3) = F_{M_x}(x_2, y_2) + Q_{y1} + H_{y1}(t), \\ m_{22}\ddot{y}_2 + m_{12}\ddot{y}_1 + m_{13}\omega(\dot{x}_1 - \dot{x}_2) + b_{y2}\dot{y}_2 + f_{y2}(x_1, \dots, \ddot{z}_3) = F_{M_y}(x_2, y_2) + Q_{y2} + H_{y2}(t), \\ m\ddot{z}_3 + b_{z3}\dot{z}_3 + f_{z3}(x_1, \dots, \ddot{z}_3) = F_{M_z}(z_3) + Q_{z3} + H_{z3}(t); \end{cases} \quad (1)$$

where  $m_{ij}$  are inertia and gyroscopic coefficients including rotor mass  $m$  and moments of inertia (equatorial  $J_1$  and polar  $J_3$  ones);  $b_{x1, \dots, z3}$  are viscosity coefficients;  $f_{x1, \dots, z3}$  are nonlinear terms of

inertia and potential field forces whose order with regard to generalised coordinates and their derivatives is comparable with that of magnetic forces dependencies (Fig. 6)  $F_{M_y}(x, y)$ ,  $F_{M_x}(x, y)$ ,  $F_{M_z}(x, y, z)$ ;  $Q_{x_1, \dots, z_3}$  are other generalised forces, in particular, force of gravity;  $H_{x_1, \dots, z_3}(t)$  are external time-dependent disturbing forces caused, in particular, by nonequilibrium.

## 2.2 Vibrograms of rotor vibrations for different rotational speeds

Computational studies were conducted for a laboratory model of a combined magnetic suspension of a rotor with the following parameters [5]:  $m = 2.5 \text{ kg}$ ,  $l_1 = 106.75 \text{ mm}$ ,  $l_2 = 176.75 \text{ mm}$ ,  $J_1 = 0.0107386 \text{ kg}\cdot\text{m}^2$ ,  $J_3 = 0.003377 \text{ kg}\cdot\text{m}^2$ ,  $\delta_r = 5.5 \text{ mm}$ ,  $\delta_a = 3 \text{ mm}$ ,  $b_{x_1 \dots y_2} = 2.325 \text{ kg}\cdot\text{s}$ ,  $e = 0.06 \text{ mm}$ ,  $\gamma = 0.003 \text{ rad}$ , and dependencies of forces  $F_{M_0}$  and  $F_{M_{z0}}$ . The Runge-Kutta fifth-order method was used for numerically solving the system of motion equations (1) for angular speed values in the range of  $0-40\pi$  with a step of  $\pi/2 \text{ rad/s}$ . For each angular speed value, the stationary solution was analysed spectrally using the Fast Fourier Transform (FFT). Fig. 7 visualises the results of such order analysis in the form of spectrograms of generalised coordinates, where  $f$  is spectrum frequency,  $\omega$  is angular speed (rotational speed), and  $A$  is amplitude of the respective generalised coordinate.

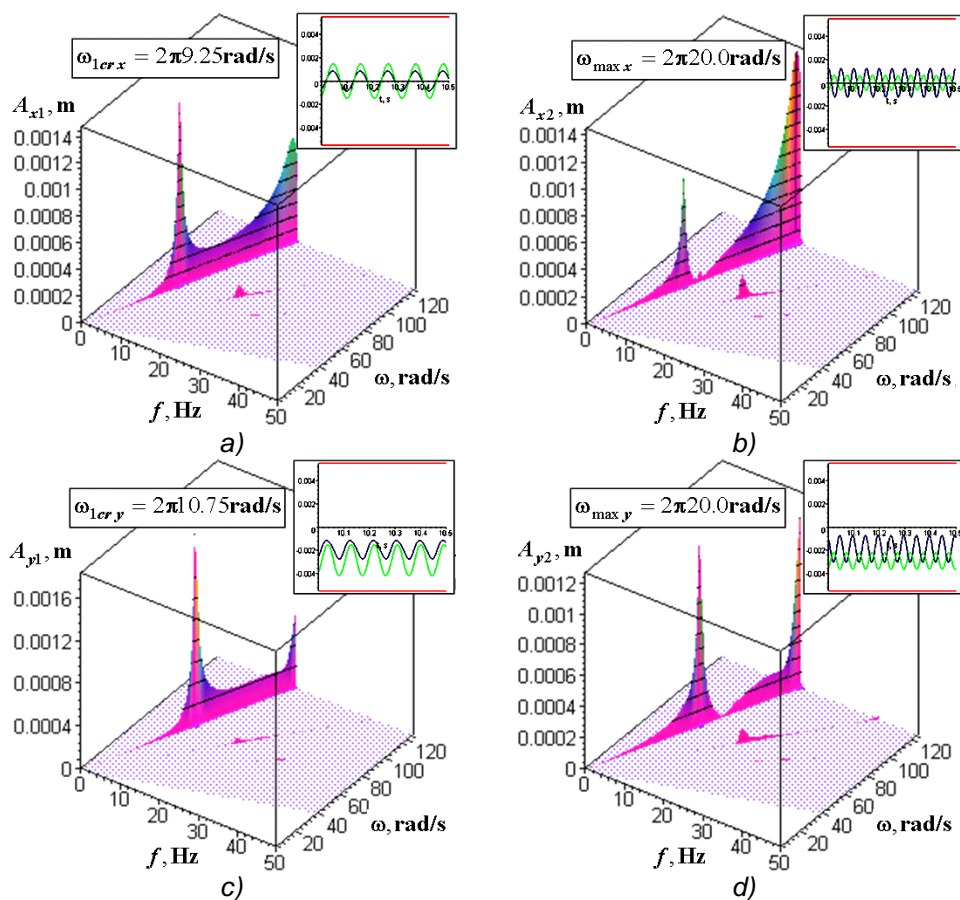


Fig. 7 Results of order analysis of rotor motion vibrograms with FFT expansion into harmonics in the direction of generalised coordinates: a)  $x_1$ , b)  $x_2$ , c)  $y_1$ , d)  $y_2$

Besides visualising the results of order analysis, the graphs show vibrograms corresponding to the first resonance mode and the end of the calculation range. It was found that the rotor motion in the first critical speed zone is of the direct cylindrical precession type (Fig. 2a). Here, the resonances during vibration in the  $x$  and  $y$  directions are displaced as per angular speed by  $9.5 \text{ rad/s}$ . Besides, these vibrations differ by the presence of superharmonics (Fig. 7). At the end of the angular speed calculation range, there is a transition to the second resonance with occurrence of subharmonics, and the rotor motion corresponds to direct conical precession (Fig. 2a). All these phenomena are in agreement with experimental studies [5]. This confirms the adequacy of the mathematical model and the validity of numerical analysis results.

## 2.3 System amplitude-frequency responses

Fig. 8 shows the first harmonic amplitudes  $A_1$  vs. field frequency dependence for generalised

coordinates  $y_1$  (light dotted line) and  $y_2$  (dark solid line) under different CS operating conditions resulting from using the force characteristics of MBPRM and AMB: operating condition I,  $F_{M0}$  and  $F_{Mz0}$ , operating condition II,  $F_{M2}$  (at  $i_{b1,2} = +3.5A$ ) and  $F_{Mz1}$ , operating condition III,  $F_{M2}$  (at  $i_{b1,2} = -3.5A$ ) and  $F_{Mz2}$ . The amplitude frequency responses corresponding to these three operating conditions are shown, respectively, in Figs. 8a, 8b and 8c. The horizontal lines show the geometrically possible deflections with account of the static equilibrium position for each coordinate. The graphs also show the motion trajectories of the rotor radial support sections in the gap for three frequency values, viz. the  $x$  resonance, the  $y$  resonance and the range end.

The AF responses shown demonstrate the possibility of passing the first critical speed when the CS is operating in design condition I without significant amplitude growth by smooth shock-free switching from one operating condition to another one according to a predesigned program, e.g., I-III-II-I (Fig. 8d).

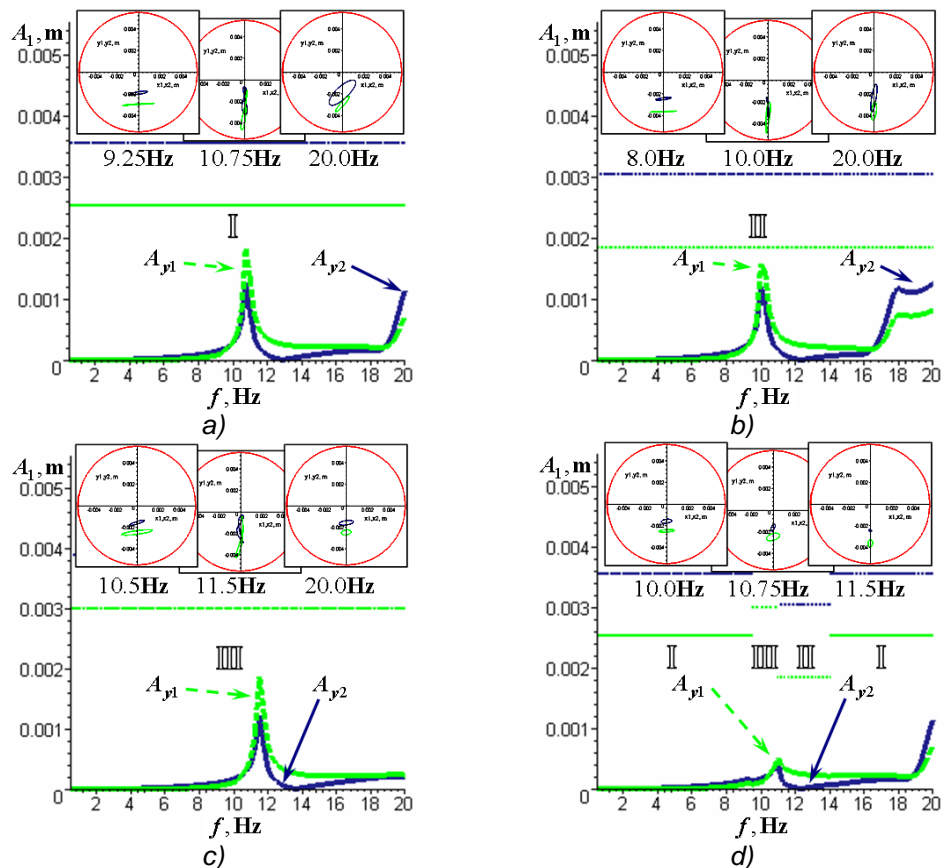


Fig. 8 Amplitude-frequency responses for first harmonic at different CS operating conditions: a) operating condition I, b) operating condition II, c) operating condition III, d) operating conditions I-III-II-I

## CONCLUSIONS

The paper shows that, by selecting the parameters of the CS of the AMB or MBPRM with a bias winding, one can ensure such force characteristics of magnetic bearings, which will prevent rotor operation in a resonance mode and in the resonance zone of any critical speed within zero to working rotational speeds. The described method of offsetting supercritical rotors from resonances and decreasing the amplitudes of resonance vibrations due to a short-time damping increase makes AMB a more preferable type of EDS as compared to other (mechanical) ones.

## REFERENCES

- [1] Kel'zon A.S. *Rotor dynamics in elastic supports*, Nauka, Moscow, 1982 (in Russian).
- [2] Schweitzer G., Bleuler H. and Traxler A. *Active magnetic bearings*, ETH, Zurich, 1994.
- [3] Martynenko G.Y. Magnetic bearings as the elastic-damping support rotors with controlled stiffness *Visnyk NTU «KhPI»*, Vol. 47, pp. 111–124, 2008 (in Russian).
- [4] G. Martynenko Modelling the dynamics of a rigid rotor in active magnetic bearings *Proceedings 6<sup>th</sup> EUROMECH Nonlinear Dynamics Conference (ENOC 2008)*, St. Petersburg, 2008.
- [5] Martynenko G. Authentication of the mathematical model of a rigid rotor on the passively-active magnetic suspension on the basis of experimental data *Mashynoznavstvo*, Vol. 12 Lviv, 2009. (in Ukrainian).